Supporting Information

Kinetics of *n*-hexane cracking over mesoporous HY zeolites based on catalyst descriptors

Yann Chapellière, Cécile Daniel, Alain Tuel, David Farrusseng, Yves Schuurman*

Mesitylene adsorption isotherms

Adsorption isotherms of mesitylene were recorded on a BELMAX (Bel Japan) at 80°C. Figure S-1 shows the adsorption isotherms for the 4 samples.

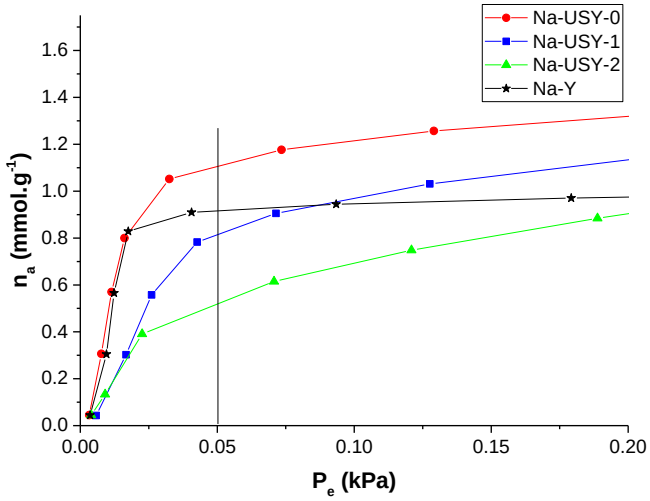

Figure S-1. *Mesitylene adsorption isotherms recorded on Belmax Japan setup at 80°C for Na-USY-0, Na-USY-1, Na-USY-2 and Na-Y.*

ZLC

Considering there is no significant external resistance to mass transfer because of the small grain size and high gas flow rates, an equilibrium between the purge gas and the sorbate at the external surface of the crystals is maintained. From Fick's diffusion equation and the mass balance consideration over the ZLC reactor, Ruthven et al. obtained the following equation for the concentration as a function of time [1]:

$$\frac{c}{c_0} = 2L \sum_{n=1}^{\infty} \frac{\exp(-\beta_n^2 Dt/r_c^2)}{\beta_n^2 + L(L-1)} \quad \text{(S-1)}$$

Where c is the adsorbate concentration, D is the diffusivity, r_c is the crystal diameter and β_n is given by:

$$\beta_n \cot \beta_n + L - 1 = 0 \quad \text{(S-2)}$$

And L:

$$L = \frac{1}{3} \times \frac{purge\ flow\ rate}{crystal\ volume} \times \frac{r_c^2}{KD} \quad \text{(S-3)}$$

In the long-time region, the large values of t simplify equation (S-3). Only the first term of the summation is significant, leading to the following expression:

$$\ln\left(\frac{c}{c_0}\right) \approx ln\left[\frac{2L}{\beta_1^2 + L(L-1)}\right] - \beta_1^2 \frac{Dt}{R^2} \quad \text{(S-4)}$$

At high flow rates, large values of L are obtained and β_1 approaches π (equation S-2 and S-3). It also implies that the intercept of the plot $c/c_0 = f(t)$ approaches 2/L and the slope, as well as the diffusion, are independent of the flow rate. These conditions, which correspond to the kinetic regime, are considered to be the best for the measurements of the intracrystalline diffusivity [1].

First the experimental regime needs to be checked. To this end, experiments are performed at several purge flows from 50 to 110 mL/min.

Under the equilibrium-controlled regime, the response curves C/C_0 should only depend on the desorption volume. It means that the plots $C/C_0 = f(F*t)$, where F corresponds to the purge flow rate and t to the desorption time, should overlap for experiments recorded at different F values [2,3]. Conversely, under the diffusion-controlled regime, the curves should diverge.

Such a plot is represented in Figure S-2 for the desorption of mesitylene from Na-USY-0 at 60°C, with purge flow rates of 50 and 100 mL/min. The partial pressure of mesitylene is 0.05 kPa and it has been adsorbed on 1.7 mg of Na-USY-0 for 2.5 h. We see the divergence of the curves obtained at 50 and 100 mL min^{-1} of helium purge flow, confirming the diffusion-controlled regime.

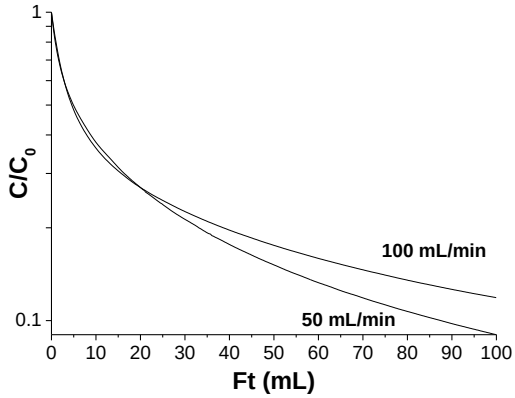

Figure S-2. *Experimental F*t plot of Na-USY-0 at 60°C with 0.05 kPa of mesitylene in nitrogen and purge flow rates of 50 and 100 mL/min.*

After this verification, experiments at several temperatures are carried out, starting from the lowest to the highest temperature. The same time for adsorption and desorption is applied. According to Silva et al. the desorption time should be higher than $7.0 \times 10^{-2} \frac{r_c^2}{D_c}$ [4]. The ZLC measurement carried out with methylene are performed with desorption of 1 h. The smallest D/R^2 coefficient is on the order of 0.5E-04 s^{-1}, which lead to a desorption time of 1400 s according to Silva et al. [4], which smaller than the applied 3600 s. Hence, the desorption time applied fulfils this criterion.

A blank test – without zeolite – is performed to determine the response time of the system.

Normalization of the signal is performed according to the equation:

$$\frac{c}{c_0} = \frac{I - I_{inf}}{I_0 - I_{inf}} \qquad \text{(S-5)}$$

Where: I is the intensity of FID signal

I_0 is the highest value after the switch from adsorption step to desorption step

I_{inf} is the value for large t. For our experiments, I_{inf} was set equal to 50.

c/c_0 is plotted as a function of the time and the exponential of equation (S-1) is fitted to the experimental data in the long-term region, leading to D/R^2 and β values. The l slope should decrease with an increase of the temperature.

ZLC curves of mesitylene desorption over Na-Y samples

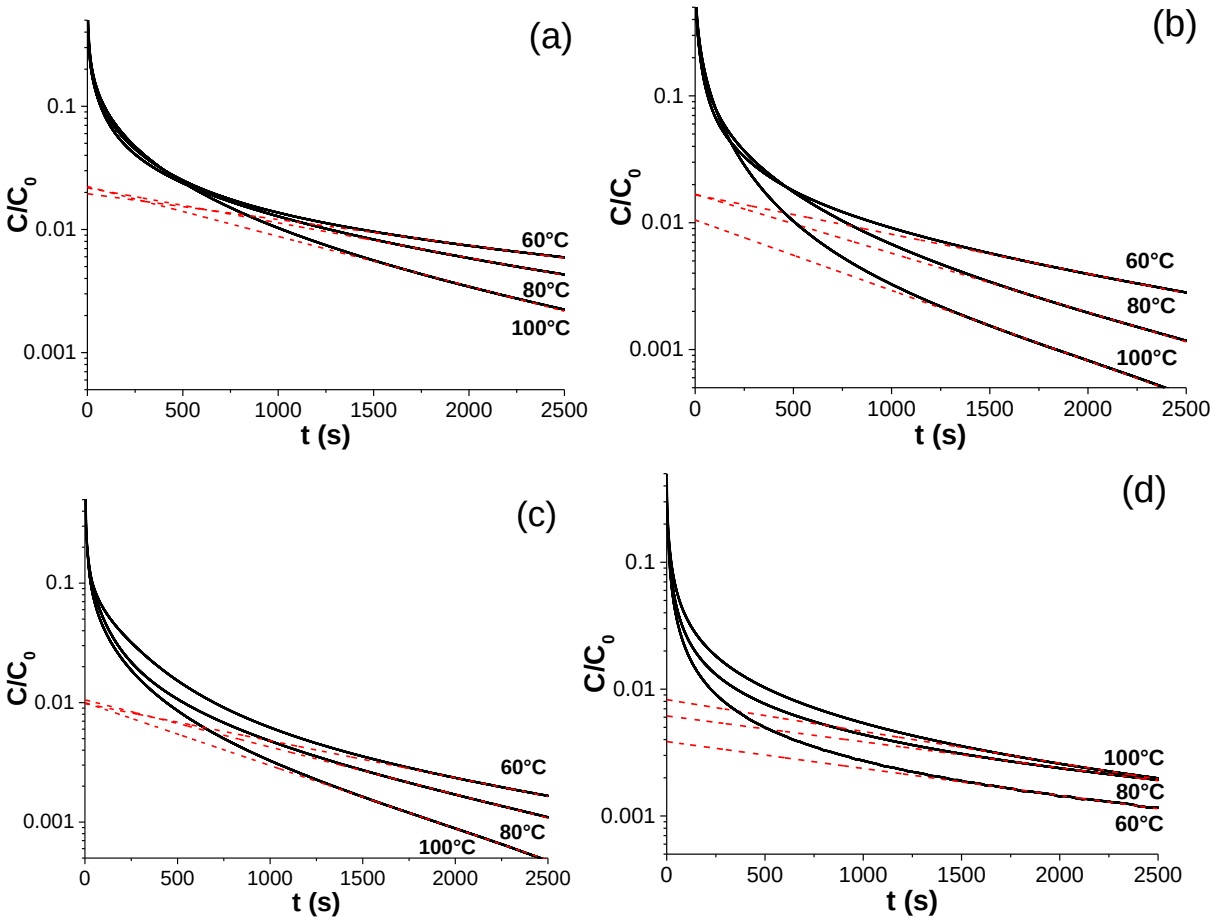

Figure S-3. *ZLC response curves for mesitylene in (a) Na-USY-0, (b) Na-USY-1, (c) Na-USY-2, (d) Na-Y at various temperatures. Red dotted lines correspond to the long-time asymptotes.*

ZLC mass balance

The flow rate of mesitylene during the adsorption phase is 1.76 µmol min^{-1}. Considering this value as the mesitylene flow rate at the beginning of the desorption phase - at $C/C_0 = 1$ - it is possible to plot the amount of mesitylene desorbed against the time of desorption (see Figure S-4). The area integration under these curves gives the amount of mesitylene desorbed during the experiments. Since ZLC measurements are carried out with 1.7 mg of catalyst, the amount of mesitylene that is desorbed per gram of Na-USY-0, Na-USY-1, Na-USY-2 and Na-Y are 0.80, 0.61, 0.35 and 0.16 mmol g^{-1}, respectively. These values are obtained after subtraction of the amount desorbed from the empty reactor.

The amount of mesitylene that is desorbed per gram of Na-USY-0, Na-USY-1, Na-USY-2 and Na-Y are 0.80, 0.61, 0.35 and 0.16 mmol g^{-1}, respectively (Figure S-4, Table S-1). These values are obtained after subtraction of the amount desorbed from the empty reactor.

It is interesting to compare these quantities to the ones obtained from the adsorption isotherms recorded at the equilibrium on the BELMAX Japan setup (Figure S-2). From isotherm measurements, the amounts of mesitylene adsorbed at 0.05 kPa, which is the partial pressure used for ZLC measurements, are 1.10, 0.81, 0.52 and 0.92 mmol g^{-1} for Na-USY-0, Na-USY-1, Na-USY-2 and Na-Y, respectively. For the first three samples, the amount of mesitylene desorbed during ZLC measurements at 80°C represents between 68 and 75% of the amount calculated at the equilibrium. These percentages are probably underestimated since the switch from the adsorption to the desorption lines disturbs the FID signal during the first two seconds of desorption. Hence, the quantities of mesitylene obtained from ZLC measurements are in good agreement with those predicted from the adsorption isotherms for samples Na-USY-0, Na-USY-1 and Na-USY-2. However, the Na-Y sample differs from the others, with less than 20% of correspondence between the two measurements. The ZLC response curves obtained for this sample, and the D/R^2 coefficients calculated from the long-time asymptotes, cannot correspond to the diffusion of the molecule through the entire crystal.

Table S-1. Comparison between ZLC and isotherm measurements.

Sample	Amount of mesitylene	
	desorbed from ZLC measurements [mmol g^{-1}]	adsorbed from isotherm measurements [mmol g^{-1}]
Na-USY-0	0.80	1.10
Na-USY-1	0.61	0.81
Na-USY-2	0.35	0.52
Na-Y	0.16	0.92

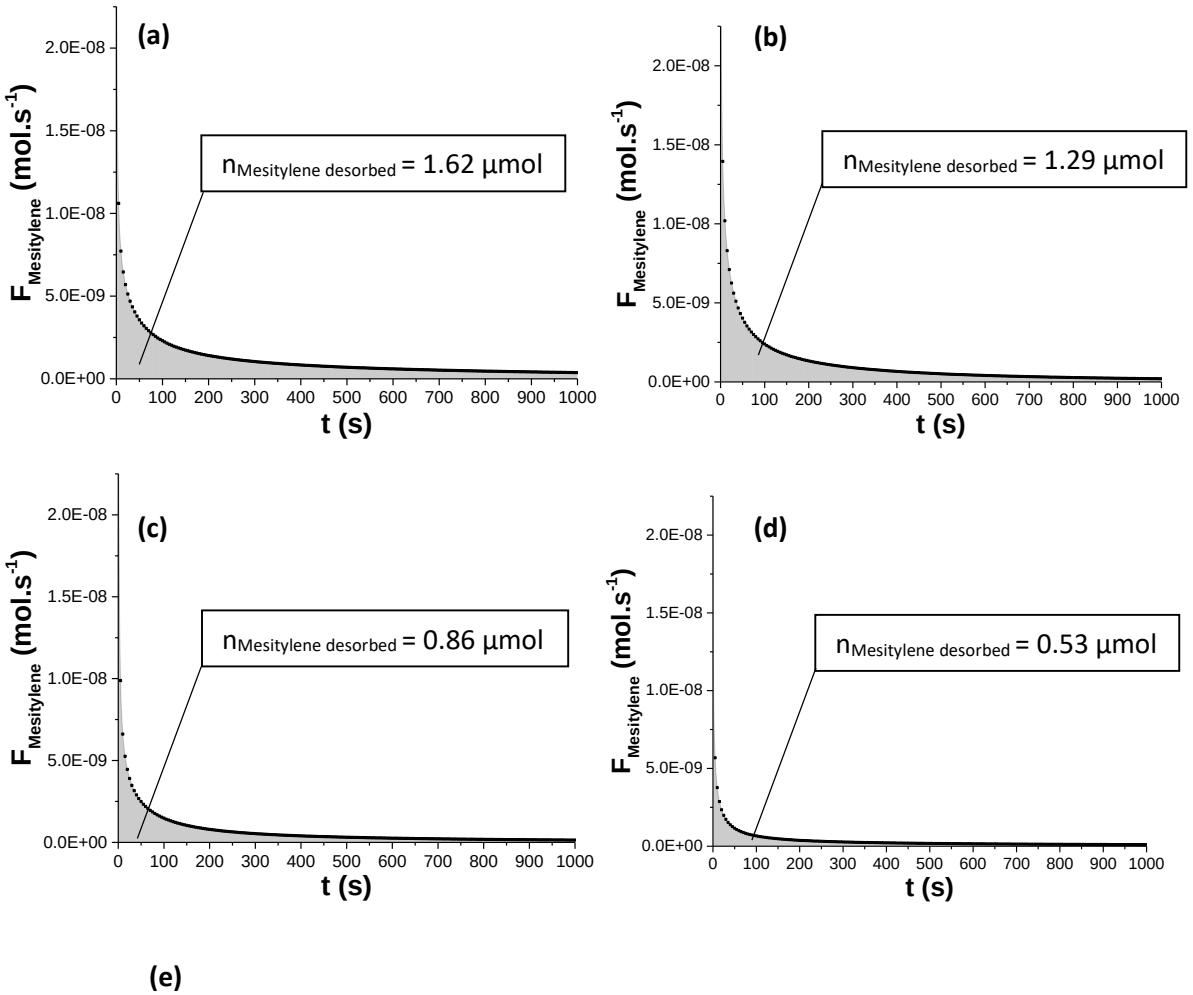

Figure S-4. *Flow of mesitylene desorbed during the desorption phase at 80°C as a function of the time for experiments carried out with (a) Na-USY-0, (b) Na-USY-1, (c) Na-USY-2 and (d) Na-Y. The surrounded boxes correspond to the number of moles of mesitylene desorbed during 2.5h and calculated from the integration of the curves.*

HR-TEM image of H-USY-2

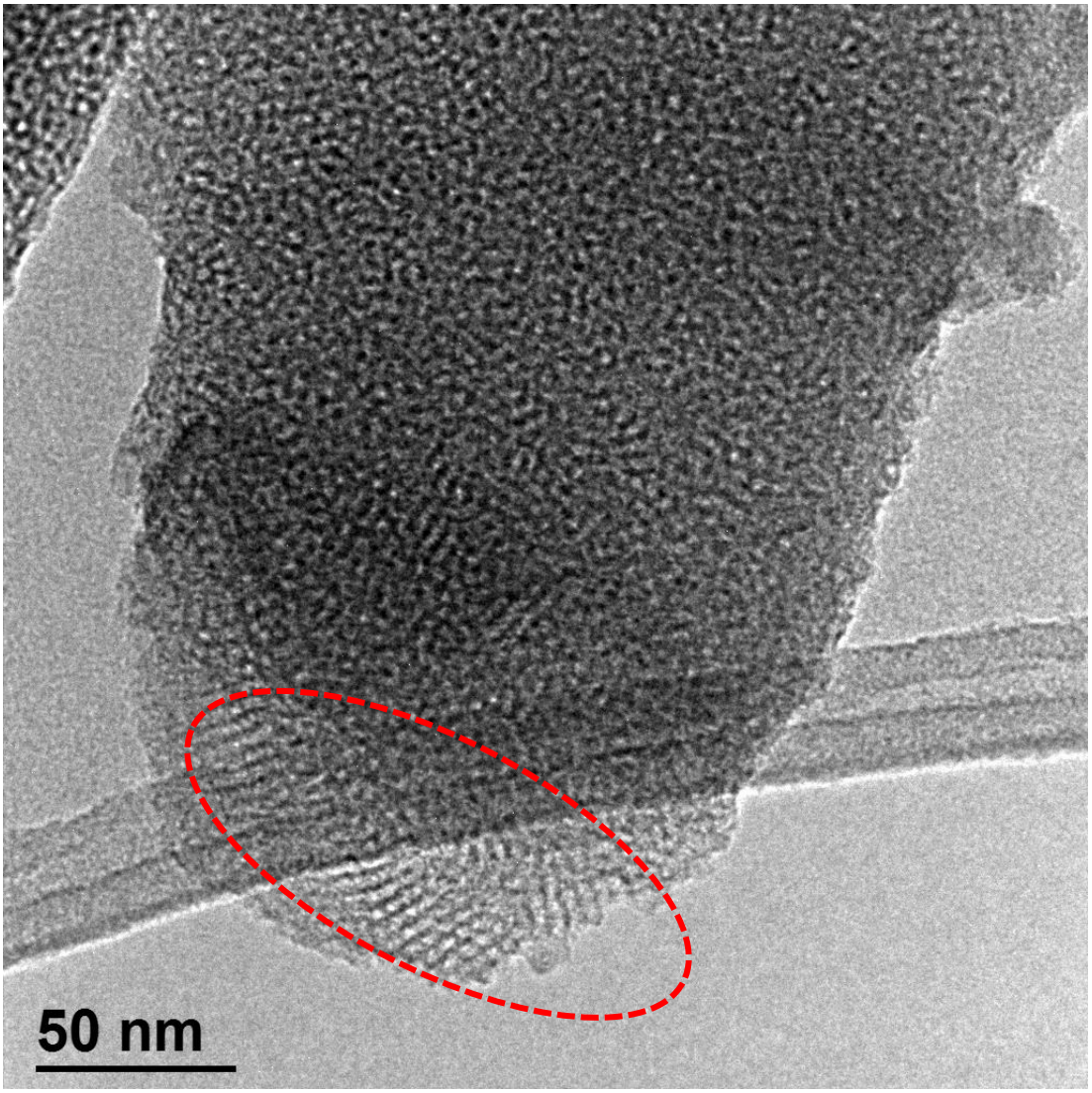

Figure S-5. *Identification of the well-organized mesoporous network of H-USY-2 sample.*

Pore size distribution by non-local density functional theory method (NLDFT)

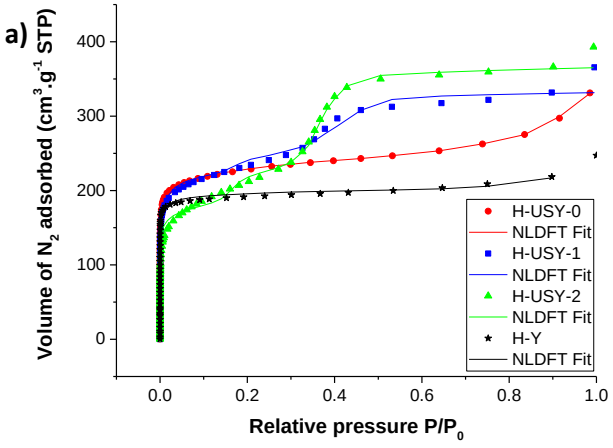

Figure S-6. *Application of NLDFT method to H-USY-0, H-USY-1, H-USY-2 and H-Y. Comparison between the NLDFT theoretical adsorption branch isotherms with experimental nitrogen adsorption isotherms.*

Nitrogen adsorption-desorption isotherm of Na-Y samples

Figure S-7 shows the volume of nitrogen adsorbed at 77K against the relative pressure p/p_0 for the Na-form zeolite.

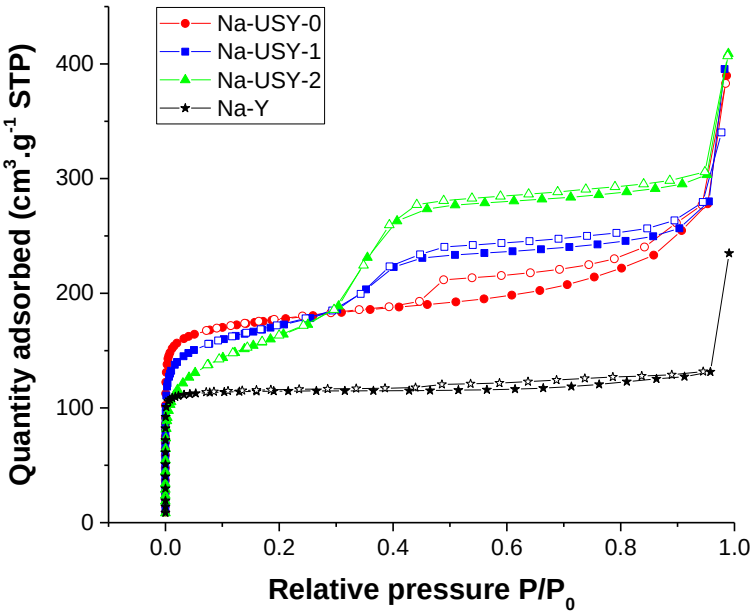

Figure S-7. N_2 adsorption-desorption isotherm at 77K of the zeolite in sodium form.

XRD of Na-Y samples

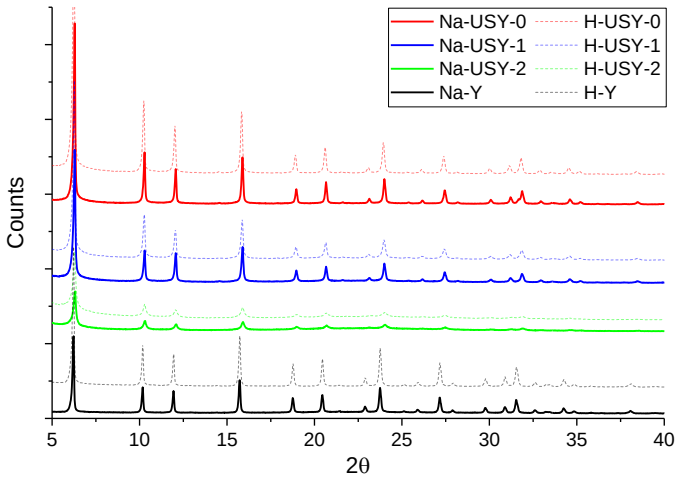

Figure S-8. *Comparison of the XRD patterns of the H and Na forms of the samples*

Table S-2: *BET surface area, micropore volume and total pore volume*

Catalyst	S_{BET} ($m^2.g^{-1}$)	V_{micro} ($cm^3.g^{-1}$)	V_{total} ($cm^3.g^{-1}$)
Na-USY-0	683	0.24	0.41
Na-USY-1	633	0.21	0.41
Na-USY-2	572	0.18	0.46
Na-Y	469	0.17	0.20

Table S-3: Elemental composition determined by ICP-OES

Sample	Si (wt. %)	Al (wt. %)	Na (wt. %)	Si/Al (molar ratio)	Na/Al (molar ratio)
Na-USY-0	37.7	2.2	2.7	16.5	1.0
Na-USY-1	37.9	2.4	0.61	15.3	0.22
Na-USY-2	37.4	2.4	0.50	15.3	0.18
Na-Y	29.0	7.9	2.4	3.5	0.26

Relative concentration of acid sites

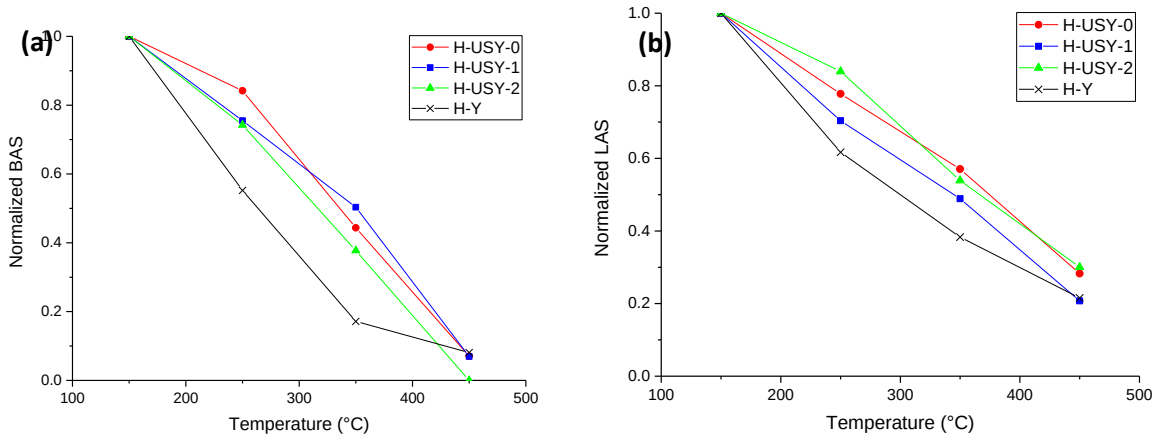

Figure S-9. *Normalized area relative to (a) Brønsted and (b) Lewis acid sites as a function of the outgassing temperature.*

FT-IR spectroscopy of pyridine adsorption

Two mains regions of the IR spectra of the zeolites are analysed. The first region to be considered is in the range of 3800-3300 cm^{-1}, corresponding to the hydroxyl groups.

The most intense peak at 3744 cm^{-1} is assigned to terminal silanol group ≡Si-(O-H) that are on the external surface of the crystals. Bridging hydroxyl groups ≡Si-(O-H)-Al≡, corresponding to the Brønsted-type acid sites, are observed at 3632 and 3567 cm^{-1}. They are assigned to the protons pointing into the supercages and the sodalite cages, respectively. Some associated bands, corresponding to these hydroxyl groups perturbed by extra framework phase, can be observed at 3603 cm^{-1} and 3525 cm^{-1}. A less intense band at 3673 cm^{-1} is attributed to hydroxyl groups present on extra framework phase. The assignations of the adsorption bands that are observed in this hydroxyl region are listed in Table S-4.

Table S-4. Assignation of the vibration bands observed in the range of 4000-3300 cm^{-1}

Wavenumber (cm^{-1})	Adsorbed species	References
3744	Terminal silanol ≡Si-(O-H)	[5,6]
3673	Hydroxyl group on extra framework species	[7]
3632	Bridging hydroxyl groups ≡Si-(O-H)-Al≡ pointing in supercages	[8]
3567	Bridging hydroxyl groups ≡Si-(O-H)-Al≡ pointing sodalite cages	[8]
3603; 3525	Bridging hydroxyl groups interacting with extraframework species	[7]

The second region of interest is in the range of 1700-1400 cm^{-1}, corresponding to the interaction between the pyridine and the surface of the material. Two bands at 1635 and 1545 cm^{-1} are assigned to the ring vibration of pyridinium ion (PyH^+). Pyridine coordinated to the zeolite leads to the vibration bands at 1621 and 1455 cm^{-1} (PyL). A fifth band, which cannot be assigned to a single site is observed at 1490 cm^{-1} [7].

Table S-5. Assignation of the vibration bands observed in the range of 1700-1400 cm^{-1} [9,10]

Wavenumber (cm^{-1})	Adsorbed species	Corresponding acid sites
1635	Pyridinium ion	Brønsted
1621	Pyridine	Lewis
1545	Pyridinium ion	Brønsted
1490	Pyridine + pyridinium ion	Lewis + Brønsted
1455	Pyridine	Lewis

The adsorption bands at 1545 and 1455 cm^{-1} are used for the calculation of the number of Brønsted and Lewis acid sites, respectively. The concentration of these acid sites, q_B and q_L, are calculated according to the following equation:

Brønsted acid site Lewis acid site

$$q_B = \frac{A_B \pi R^2}{w \varepsilon_B} \qquad q_L = \frac{A_L \pi R^2}{w \varepsilon_L} \qquad (1)$$

Where A_B and A_L are the area of the adsorption bands at 1545 and 1455 cm^{-1} [cm^{-1}], R is the radius of the wafer [cm], w is the weight of the sample [g] and ε_B and ε_L are the integrated extinction coefficients for Brønsted and Lewis acid sites.

The extinction coefficients should be determined by introducing a known amount of the probe molecule into the cell. The progressive change in intensity for the considered band as a function of the amount of probe introduced into the cell allows determining the integrated molar adsorption. This method needs the introduction of a carefully calibrated amount of pyridine, which is not possible in our case. Such coefficients have already been determined by other research groups and are widely used in the literature. The integrated extinction coefficients from C. A. Emeis work, ε_B=1.67 cm μmol^{-1} and ε_L=2.22 cm μmol^{-1}, are chosen for the calculations of the equations (8) [11]. The strength of acid sites is investigated by normalization of the number of acid sites obtained after desorption of the pyridine at 150°C.

Product distribution of n-hexane cracking

Figure S-10 displays the selectivity obtained for each reaction product as a function of the conversion. The selectivity values for the C_5, $C_5^=$, C_6 and benzene are lower than 1%. For a clarity purpose they are not displayed. The main reaction product obtained with the four catalysts is propylene. Regardless of the reaction temperature, or the n-hexane conversion, propylene accounts for between 35% - 40% of the products of reaction. For the other reaction products, only slight differences appear depending of the catalyst. With H-USY-0 and H-USY-1, propane is the second main reaction product, followed by ethane. The selectivity of these two products tends to decrease when increasing the reaction temperature. In opposite, the hydrogen selectivity tends to increase, as well as the ethylene and methane ones. For the cracking reaction over H-USY-2 and H-Y, the selectivity of ethane is higher than propane. The hydrogen selectivity seems constant with reaction temperature.

The thermal cracking is investigated with experiments carried out without catalyst. Conversion of n-hexane is only detected at 650°C. At this temperature, 3.7% of the reactant is converted, into mainly C_1 (17.6%), $C_2^=$ (26.2%), C_2 (20.2%) and $C_3^=$ (16.5%).

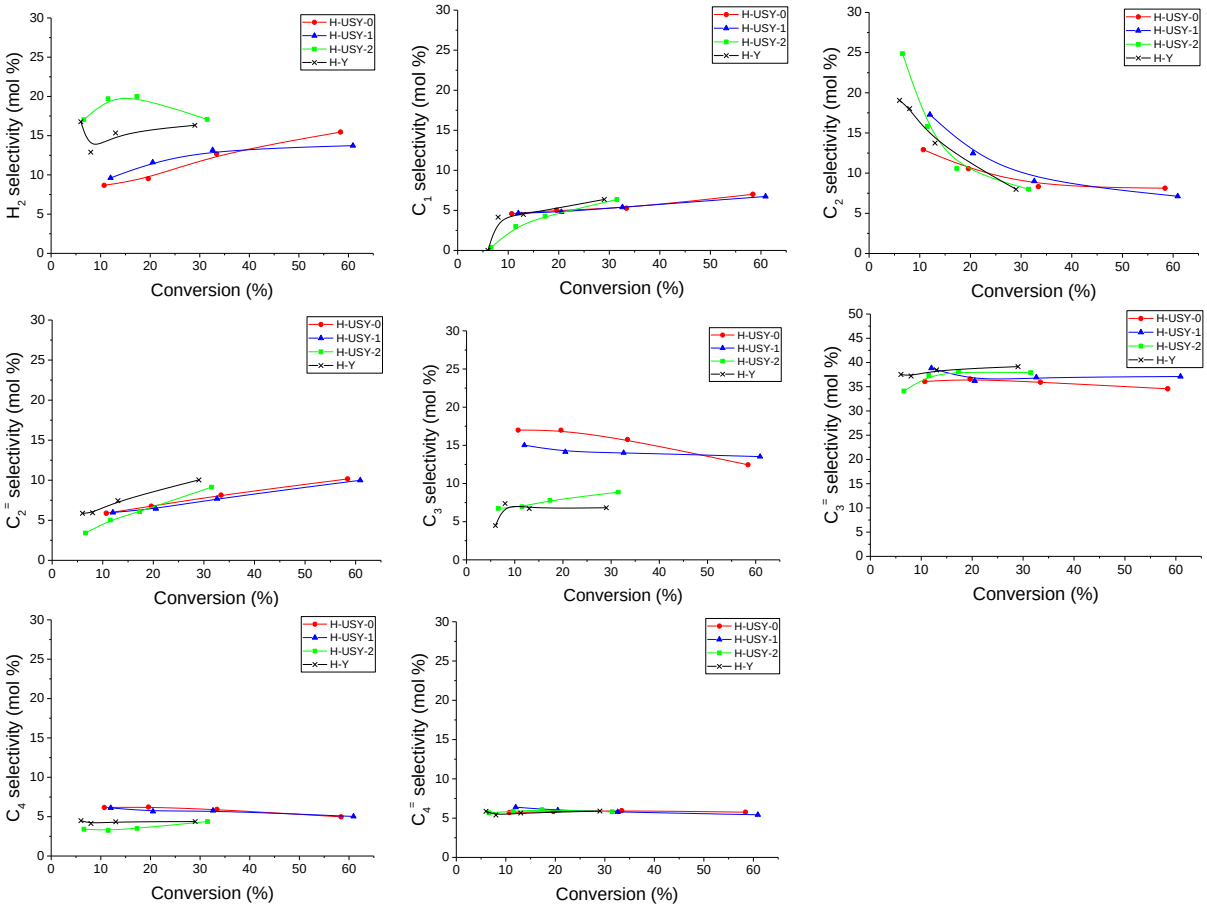

Figure S-10. *Selectivity of H_2, C_1, C_2, $C_2^=$, C_3, $C_3^=$, C_4, $C_4^=$ for C_2+C_3+C_4+C_5 products as a function of the conversion for the catalytic cracking of n-hexane on H-USY-0, H-USY-1, H-USY-2 and H-Y.*

TAP n-hexane pulse responses modeling.

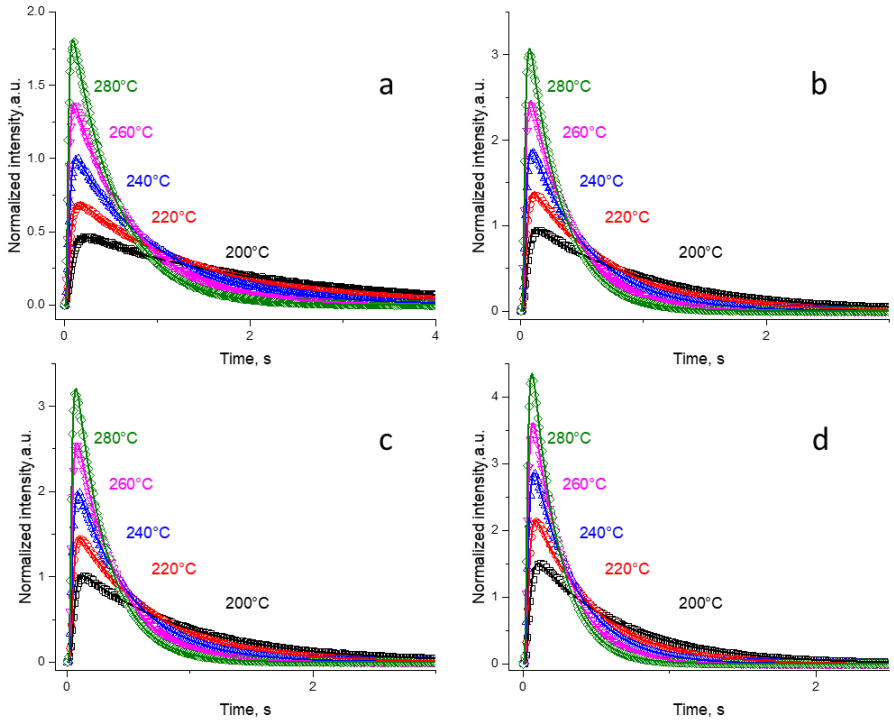

Figure S-11. *TAP normalized pulse response of n-hexane (symbols) compared to model predictions (full line) at 200, 220, 240, 260 & 280°C. a: H-Y, b: H-USY-0, c: H-USY-1, d: H-USY-2.*

References

[1] J. Kärger, D. M. Ruthven, and D. N. Theodorou, *Diffusion in Nanoporous Materials*. 2012.

[2] X. Hu, E. Mangano, D. Friedrich, H. Ahn, and S. Brandani, "Diffusion mechanism of CO2 in 13X zeolite beads," *Adsorption*, vol. 20, no. 1, pp. 121–135, 2014, doi: 10.1007/s10450-013-9554-z.

[3] S. Brandani, "A Simple Graphical Check of Consistency for Zero Length Column Desorption Curves," *Chem. Eng. Technol.*, vol. 39, no. 6, pp. 1194–1198, 2016, doi: 10.1002/ceat.201500634

[4] J. A. C. Silva and A. E. Rodrigues, "Limitations of the Zero-Length Column Technique to Measure Diffusional Time Constants in Microporous Adsorbents," *Chem. Eng. Technol.*, vol. 38, no. 12, pp. 2335–2339, 2015

[5] L. E. Sandoval-Diaz, J. A. Gonzalez-Amaya, and C. A. Trujillo, "General aspects of zeolite acidity characterization," Microporous Mesoporous Mater., vol. 215, pp. 229–243, 2015

[6] V. Rac, D. Stošić, V. Rakić, and A. Auroux, "Acidity of Hierarchical Fau , Bea and Zsm-5 Zeolites," pp. 140–143.

[7] T. Barzetti, E. Selli, D. Moscotti, and L. Forni, “Pyridine and ammonia as probes for FTIR analysis of solid acid catalysts,” J. Chem. Soc. Faraday Trans., vol. 92, no. 8, p. 1401, 1996.

[8] J. A. Lercher and A. Jentys, “Chapter 13 - Infrared and raman spectroscopy for characterizing zeolites,” in Introduction to Zeolite Science and Practice, vol. 168, 2007, pp. 435–476.

[9] W. Daniell, N. Y. Topsøe, and H. Knözinger, “An FTIR study of the surface acidity of USY zeolites: Comparison of CO, CD3CN, and C5H5N probe molecules,” Langmuir, vol. 17, no. 20, pp. 6233–6239, 2001.

[10] E. P. Parry, “An Infrared Study of Pyridine Adsorbed on Acidic Solids. Characterization of Surface Acidity,” J. Catal., vol. 2, pp. 371–379, 1963.

[12] C. A. Emeis, “Determination of integrated molar extinction coefficients for infrared absorption bands of pyridine adsorbed on solid acid catalysts,” Journal of Catalysis, vol. 141, no. 2. pp. 347–354, 1993.